Differentiated Parkinson patient-derived induced pluripotent stem cells grow in the adult rodent brain and reduce motor asymmetry in Parkinsonian rats

Citation: Hargus, G., O. Cooper, M. Deleidi, A. Levy, K. Lee, E. Marlow, A. Yow, et al. "Differentiated Parkinson patient-derived induced pluripotent stem cells grow in the adult rodent brain and reduce motor asymmetry in Parkinsonian rats." Proceedings of the National Academy of Sciences 107, no. 36 (September 7, 2010): 15921-15926.

As Published: http://dx.doi.org/10.1073/pnas.1010209107

Publisher: National Academy of Sciences (U.S.)

Persistent URL: http://hdl.handle.net/1721.1/84625

Version: Final published version: final published article, as it appeared in a journal, conference proceedings, or other formally published context

Differentiated Parkinson patient-derived induced pluripotent stem cells grow in the adult rodent brain and reduce motor asymmetry in Parkinsonian rats

Gunnar Hargus[a], Oliver Cooper[a], Michela Deleidi[a], Adam Levy[a], Kristen Lee[a], Elizabeth Marlow[a], Alyssa Yow[a], Frank Soldner[b], Dirk Hockemeyer[b], Penelope J. Hallett[a], Teresia Osborn[a], Rudolf Jaenisch[b,1], and Ole Isacson[a,1]

[a]Udall Parkinson's Disease Research Center of Excellence and Center for Neuroregeneration Research, McLean Hospital/Harvard Medical School, Belmont, MA 02478; and [b]Whitehead Institute for Biomedical Research, Massachusetts Institute of Technology, Cambridge, MA 02142

Contributed by Rudolf Jaenisch, July 14, 2010 (sent for review April 15, 2010)

Recent advances in deriving induced pluripotent stem (iPS) cells from patients offer new possibilities for biomedical research and clinical applications, as these cells could be used for autologous transplantation. We differentiated iPS cells from patients with Parkinson's disease (PD) into dopaminergic (DA) neurons and show that these DA neurons can be transplanted without signs of neurodegeneration into the adult rodent striatum. The PD patient iPS (PDiPS) cell-derived DA neurons survived at high numbers, showed arborization, and mediated functional effects in an animal model of PD as determined by reduction of amphetamine- and apomorphine-induced rotational asymmetry, but only a few DA neurons projected into the host striatum at 16 wk after transplantation. We next applied FACS for the neural cell adhesion molecule NCAM on differentiated PDiPS cells before transplantation, which resulted in surviving DA neurons with functional effects on amphetamine-induced rotational asymmetry in a 6-OHDA animal model of PD. Morphologically, we found that PDiPS cell-derived non-DA neurons send axons along white matter tracts into specific close and remote gray matter target areas in the adult brain. Such findings establish the transplantation of human PDiPS cell-derived neurons as a long-term in vivo method to analyze potential disease-related changes in a physiological context. Our data also demonstrate proof of principle of survival and functional effects of PDiPS cell-derived DA neurons in an animal model of PD and encourage further development of differentiation protocols to enhance growth and function of implanted PDiPS cell-derived DA neurons in regard to potential therapeutic applications.

cell replacement therapy | dopaminergic neurons | Parkinson's disease | reprogramming | transplantation

The induced pluripotent stem (iPS) cell technology provides an opportunity to generate cells with characteristics of embryonic stem (ES) cells, including pluripotency and potentially unlimited self-renewal (1). During the past few years, several studies have reported a directed differentiation of iPS cells into a variety of functional cell types in vitro, and cell therapy effects of implanted iPS cells have been demonstrated in several animal models of disease (2, 3).

Reprogramming technology has been applied to derive patient-specific iPS cell lines, which carry the identical genetic information as their patient donor cells. This is particularly interesting for regenerative cell therapy approaches, as differentiated patient-specific iPS cells might be used for autologous transplantation. Patient-specific iPS cell lines have been generated for several diseases, including hematologic (4), metabolic (5, 6), and neurologic disorders (5, 7–9). To model disease in vitro, changes have been obtained in patient-derived iPS cells, which could be modified through the application of chemical compounds during iPS cell differentiation (8, 9) or prevented by gene targeting before iPS cell derivation (4). Furthermore, functional phenotypes such as insulin-producing cells from diabetic patients have been generated from iPS cells in vitro (6), demonstrating that patient-derived iPS cells can constitute a potential source for future clinical applications.

Cell replacement therapy is promising in diseases with a relatively selective cell loss, such as Parkinson's disease (PD), in which dopaminergic (DA) neuron degeneration is responsible for motor symptoms in patients. Several studies have shown that some patients with PD benefit from the transplantation of human fetal cells (10, 11), but limited tissue availability requires alternative cellular sources. Human ES (hES) cells have been transplanted into animal models of PD after in vitro differentiation into neural precursors (12) or DA neurons (13, 14), and partial functional recovery was observed in some of these reports (12, 13). One study reported complete functional recovery after transplantation of differentiated hES cells but severe graft overgrowth was found in engrafted animals (15), emphasizing efforts to purify hES cell-derived neurons via FACS before transplantation (16, 17).

We have recently derived several iPS cell lines from patients with idiopathic PD, which are able to differentiate into DA neurons in vitro (7). Here, we applied a series of transplantation experiments on these PDiPS cell lines to first investigate the development and integration of PD patient iPS (PDiPS) cell-derived neurons in vivo and second to analyze if PDiPS cell-derived DA neurons can function in an animal model of PD.

Results

PDiPS Cells Differentiate into DA Neurons in Vitro and Survive After Transplantation into the Adult Striatum of Unlesioned Rats. We have generated several PDiPS cell lines by transduction of dermal fibroblasts with DOX-inducible lentiviruses encoding oct4, klf4, and sox2 and have described in vitro characteristics of pluripotency and differentiation in these lines (7). We used two PDiPS cell lines, in which the reprogramming factors had been excised after reprogramming (FF17-5 and FF21-26 PDiPSCs; Table 1) (7). In addition, two different PDiPS cell lines from two other patients with PD were used, in which the reprogramming factors were present but their expression not induced (K1 and S1 PDiPS cells; Table 1) (7).

We first analyzed the potential of the four PDiPS cell lines to differentiate into DA neurons in vitro (Fig. S1) using the stromal feeder cell-based differentiation protocol (14, 18). Consistent with our previously published findings from other PDiPS cell lines (7), we did not observe major differences in DA differentiation when comparing the factor-carrying and the factor-free PDiPS cells with hES cells or non-PDiPS cells that had been derived from a subject who did not have PD (Fig. S1). However, one of the PDiPS

Author contributions: G.H., R.J., and O.I. designed research; G.H., O.C., M.D., A.L., K.L., E.M., A.Y., F.S., D.H., and T.O. performed research; F.S., D.H., and O.I. contributed new reagents/analytic tools; G.H., O.C., M.D., A.L., P.J.H., and O.I. analyzed data; and G.H., R.J., and O.I. wrote the paper.

The authors declare no conflict of interest.

[1]To whom correspondence may be addressed. E-mail: jaenisch@wi.mit.edu or isacson@hms.harvard.edu.

This article contains supporting information online at www.pnas.org/lookup/suppl/doi:10.1073/pnas.1010209107/-/DCSupplemental.

Table 1. Summary of cell lines analyzed in this study

ES/iPS cells studied	H9	A6	K1	S1	FF 17–5	FF 21–26
Cell type	hESC	Non-PDiPSC	PDiPSC	PDiPSC	PDiPSC	PDiPSC
Original cell code (7)	H9	iPS A6	iPS PDA^{3F}-1	iPS PDC^{3F}-1	PDB^{3F}-17Puro-5	PDB^{3F}-21Puro-26
Parental cell line*	—	GM 01660	AG 20443	AG 20446	AG 20442	AG 20442
Dox-inducible lentivirus	—	Yes	Yes	Yes	Yes	Yes
Reprogramming factors	—	Oct4	Oct4	Oct4	Oct4	Oct4
	—	Klf4	Klf4	Klf4	Klf4	Klf4
	—	Sox2	Sox2	Sox2	Sox2	Sox2
Excision of reprogramming factors	—	No	No	No	Yes	Yes
	—	—	—	—	Factor-free	Factor-free

*Coriell Institute code.

cell lines (S1 PDiPSC) showed an enhanced overall neuronal differentiation but no tendency toward enhanced DA differentiation at day 42 in vitro (Fig. S1). In all stem cell lines, less than 1% of all tyrosine hydroxylase (TH)-positive neurons coexpressed dopamine-β-hydroxylase (DBH), showing that the vast majority of TH$^+$ neurons were DA, and not noradrenergic, neurons.

Next, differentiated K1, S1, FF17-5, and FF21-26 PDiPS cells were transplanted into the striatum of unlesioned rats to analyze if engrafted PDiPS cell-derived DA neurons could survive in the adult brain. Four weeks after transplantation, engrafted cells were visualized through a staining against the neural cell adhesion molecule NCAM using a human-specific antibody (Fig. 1*A*). Viable grafts were found at the expected stereotaxic position in 25 of 26 animals and the mean volumes of the grafts were 0.26 ± 0.03 mm^3 (K1), 0.60 ± 0.18 mm^3 (S1), 1.60 ± 0.56 mm^3 (FF17-5), and 0.44 ± 0.05 mm^3 (FF21-26). Observed differences in these small graft sizes were most likely a result of variabilities in cell preparation and cell batches for transplantation, as cells from one single differentiation batch were implanted for each PDiPS cell group. Grafts from all four PDiPS cell lines contained human NCAM (hNCAM)-positive and TH$^+$ DA neurons at a mean density of 122 ± 24 DA neurons per mm^3, which were located at the center and periphery of the transplants (Fig. 1*B*). To analyze longer survival times, we retained five rats with engrafted K1 PDiPS cells and five rats with FF21-26 PDiPS cells from the same series for an additional 8 wk. In all 10 animals, we found viable grafts with DA neurons (Fig. 1 *C* and *D*). Some of these DA neurons stained positive for Girk-2, which is coexpressed with TH in mesencephalic DA neurons (Fig. 1 *C* and *D*). Next, the PDiPS cell grafts were stained for βIII-tubulin, ubiquitin, and α-synuclein to analyze if engrafted neurons showed any signs of inclusion body formation. We did not detect any ubiquitin-positive and α-synuclein–positive inclusion bodies in PDiPS cell-derived DA and non-DA neurons in any of the grafts analyzed up to 12 wk after transplantation.

The transplantation of differentiated PDiPS cells induced a very modest astrogliosis around the grafts (Fig. 1*E*). A small number of engrafted cells was found to be GFAP-positive astrocytes (Fig. 1*E*), whereas the expression of the neural cell adhesion molecule L1, expressed on postmitotic neurons, was abundant in the grafts (Fig. 1*F*). None of the 36 rats engrafted with differentiated K1, S1, FF17-5, and FF21-26 PDiPS cells showed signs of tumor formation up to 12 wk after transplantation.

Engrafted PD Patient-Derived Neurons Send out Non-DA Axonal Projections to Close and Remote Target Areas in the Adult Unlesioned Rodent Brain. Given that the majority of the neurons in PDiPS cell grafts are non-DA, we investigated other than DA neuronal cell types in the grafts using this in vivo bioassay. For comparison, differentiated non-PDiPS cells and hES cells were transplanted into the striatum of unlesioned rats, and grafts were analyzed 4 wk after transplantation. As an indirect way to analyze non-DA neuronal phenotypes within the grafts, we followed the fiber outgrowth of hNCAM$^+$ neurons throughout the adult rodent brain since engrafted neurons are known to project to their target areas according to their intrinsic phenotypic de-

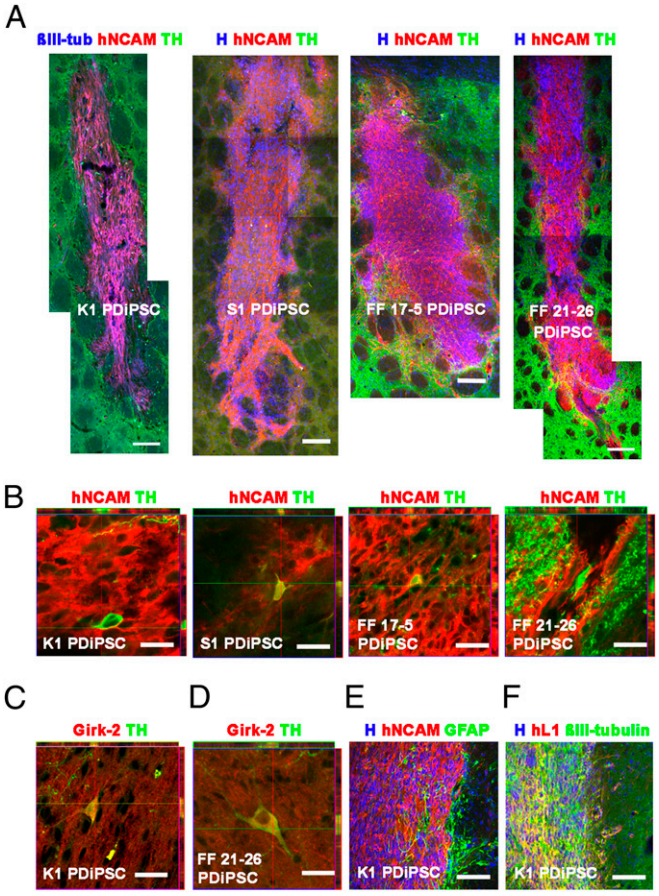

Fig. 1. PD patient-derived DA neurons survive after transplantation into the adult striatum of unlesioned rats. (*A*) Assembled images of K1, S1, FF 17–5, and FF 21–26 PDiPS cell grafts immunostained for human NCAM (red), TH (green), βIII-tubulin (blue), or Hoechst (H; blue) 4 wk after intrastriatal transplantation of 200,000 cells. A high number of neurons was present in all grafts. (*B*) Z-stacks of three confocal images of 1 μm thickness show coexpression of TH (green) and hNCAM (red) in engrafted DA neurons derived from all four PDiPS cell lines 4 wk after transplantation. (*C* and *D*) Stacked confocal images of DA neurons coexpressing Girk-2 (red) and TH (green) 12 wk after transplantation. (*E*) Immunostaining for hNCAM (red), GFAP (green), and H (blue) showing moderate astrogliosis around grafts. (*F*) Immunostaining for human L1 (red), βIII-tubulin (green) and H (blue) showing a high number of neurons at the graft–host interface. (Scale bars: 100 μm in *A*, *E*, and *F*; 20 μm in *B*–*D*.)

termination, as previously shown in several xenografting experiments (19–21). Grafts consisting of all PDiPS cell lines or control lines contained hNCAM$^+$ cells, which sent projections to the surrounding gray and white matter (Fig. 2 and Fig. S2). The neurite outgrowth pattern was examined systematically in all six groups, and specific and reproducible patterns were found within each group. These outgrowth patterns were similar for the four PDiPS cell, the non-PDiPS cell, and the hES cell groups (Fig. 2 *A*–*R*). A complete list of gray matter zone target areas is shown in Table S1.

As some neurite outgrowth patterns were reminiscent of an outgrowth pattern of cortical projection neurons, we analyzed the expression of the cortical transcription factor bhlhb5 in the grafts 4 wk after transplantation (Fig. 2 *S*–*U*). In all groups, we found small groups of bhlhb5$^+$ and hNCAM$^+$ cortical neurons

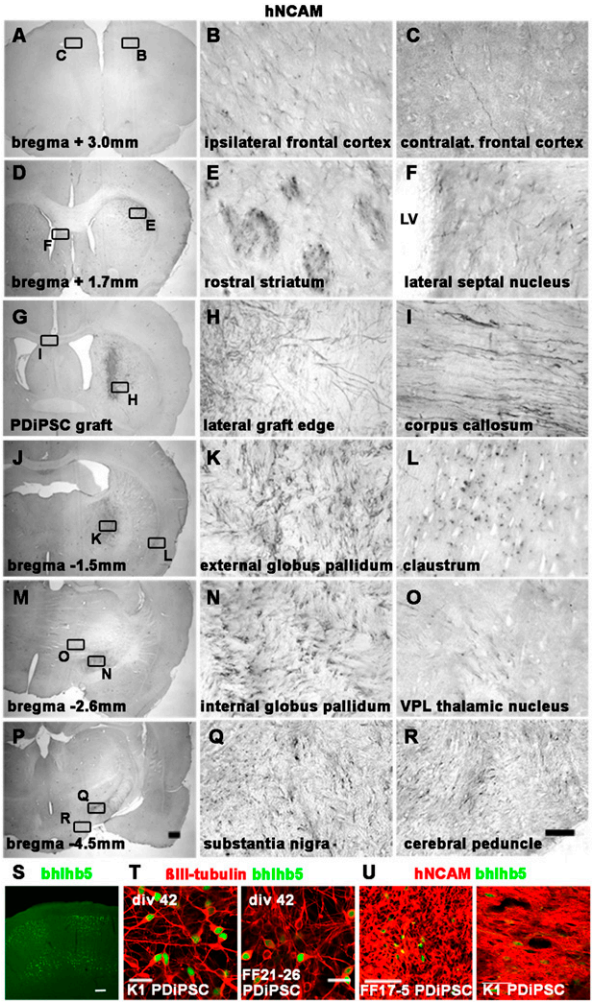

Fig. 2. Engrafted PD patient–derived neurons send out fibers to close and remote target areas in the adult unlesioned rodent brain. (*A*–*R*) Photomicrographs of hNCAM-stained brain sections 4 wk after engraftment of S1 PDiPS cells representing the axonal outgrowth pattern of engrafted PDiPS cell-, non-PDiPS cell–, and hES cell-derived neurons. Graft-derived axons project along white matter tracts (*E*, *I*, and *R*) to specific gray matter zone target areas in the adult rodent brain. The boxed areas (*Left*) are also shown in higher magnification (*Right*). (Scale bars: 25 μm, *Right*; 500 μm, *Left*.) LV, lateral ventricle; VPL, ventroposterolateral. (*S*) Immunostaining of the adult rat somatosensory cortex for the cortical marker bhlhb5. (Scale bar: 100 μm.) (*T*) Immunostainings of differentiated PDiPS cells at day 42 in vitro for βIII-tubulin (red) and bhlhb5 (green). (Scale bar: 20 μm.) (*U*) Immunostainings of differentiated PDiPS cells for hNCAM (red) and bhlhb5 (green) 4 wk after transplantation. (Scale bar: 50 μm.)

(<1%), but we did not detect any differences in bhlhb5 expression between the PDiPS, the non-PDiPS, and the hES cell grafts.

The lack of differences in donor axon target patterns among the six groups led us to analyze quantitative changes in graft-derived hNCAM$^+$ fibers within the different target areas in the host brain. Therefore, we determined the fiber outgrowth per area in 40-μm brain sections as listed in Table S1. Although slight differences were found in distinct brain areas among the six groups, we did not detect any patterns that indicated PD cell- or iPS cell–specific changes in axonal outgrowth or density between the cell lines.

Analysis of PDiPS Cell-Derived DA Neurons in 6-hydroxydopamine–Lesioned Rats. As the engrafted PDiPS cell-derived DA neurons survive in the adult rodent brain for at least 12 wk, we next transplanted differentiated S1 PDiPS cells into the dorsolateral striatum of 6-hydroxydopamine (6-OHDA)–lesioned rats (n = 12), which serve as an animal model of PD, and grafts were analyzed histologically 16 wk after transplantation (Fig. 3). As in the previously described bioassays, the grafts were located at the expected stereotaxic position except for one graft that reached into the globus pallidum (Fig. 3*B*). All grafts contained a high number of DA neurons (4,890 ± 640) that were distributed throughout the grafts (Fig. 3 *A*–*F*). Consistent with our in vitro data, less than 1% of TH$^+$ neurons coexpressed DBH as a marker for noradrenergic neurons (Fig. 3*N*). The engrafted DA neurons sent TH$^+$ fibers toward other cells within the grafts and some of the DA neurons showed intense arborization and branching (Fig. 3 *C*–*E*).

We next analyzed the outgrowth of DA neurons at the graft/host interface and found that only few donor-derived DA neurons sent their axons toward the DA-depleted host striatum (Fig. 3*G*). We also analyzed if an astroglial or a microglial reaction was present around the grafts as such reactions could influence graft/host connectivity. Only a small number of astroglial and microglial cells was found around the grafts (Fig. 3 *H* and *I*).

Next, engrafted DA neurons were stained for the midbrain DA neuronal markers Girk-2 and calbindin (Fig. 3 *J*–*L*). As seen in the in vivo bioassays, we found TH- and Girk-2–coexpressing DA neurons within the grafts (Fig. 3 *J* and *L*). Such neurons accounted for 53.4 ± 6.6% of all engrafted DA neurons (Fig. 3*M*). In addition, TH$^+$ and calbindin-positive DA neurons were also present in the grafts (6.6 ± 0.2% of all engrafted DA neurons; Fig. 3 *J*, *K*, and *M*). Furthermore, the grafts contained a small number of TH$^+$ and GABA$^+$ forebrain DA neurons (4.7 ± 1.0%) and TH$^+$ and Nkx2.1$^+$ hypothalamic DA neurons (5.8 ± 1.2%). An immunostaining for TH and α-synuclein showed that the engrafted DA neurons did not contain any α-synuclein–positive inclusion bodies (Fig. 3 *O*–*Q*). Instead, a punctate synaptic expression pattern of α-synuclein was found in donor-derived neurons within the grafts and also in the host striatum.

None of the 12 animals with S1 PDiPS cell grafts showed signs of tumor formation, and the mean size of the grafts was 1.1 ± 0.08 mm^3. Among all engrafted cells, 0.09 ± 0.02% were positive for the proliferative marker Ki-67 and 83.1 ± 8.2% of these cells coexpressed hNCAM. Neither SSEA-4- nor oct4-expressing cells were found in the grafts 16 wk after transplantation.

Reduced Motor Asymmetry of 6-OHDA–Lesioned Rats After Intrastriatal Transplantation of differentiated PDiPS Cells. To analyze if the PDiPS cell-derived DA neurons were also functional in vivo, rotational tests, a cylinder test, and an adjustment stepping test were performed on all 12 transplanted rats, and their behavioral performance was compared with 6-OHDA–lesioned control rats that had not received any transplants (n = 9; Fig. 4). Before surgery, all rats showed severe motor asymmetry induced by both DA agonists, which did not improve in control rats over time (Fig. 4 *A* and *D*). In contrast, PDiPS cell-transplanted rats showed a progressive reduction in ipsilateral amphetamine-induced ro-

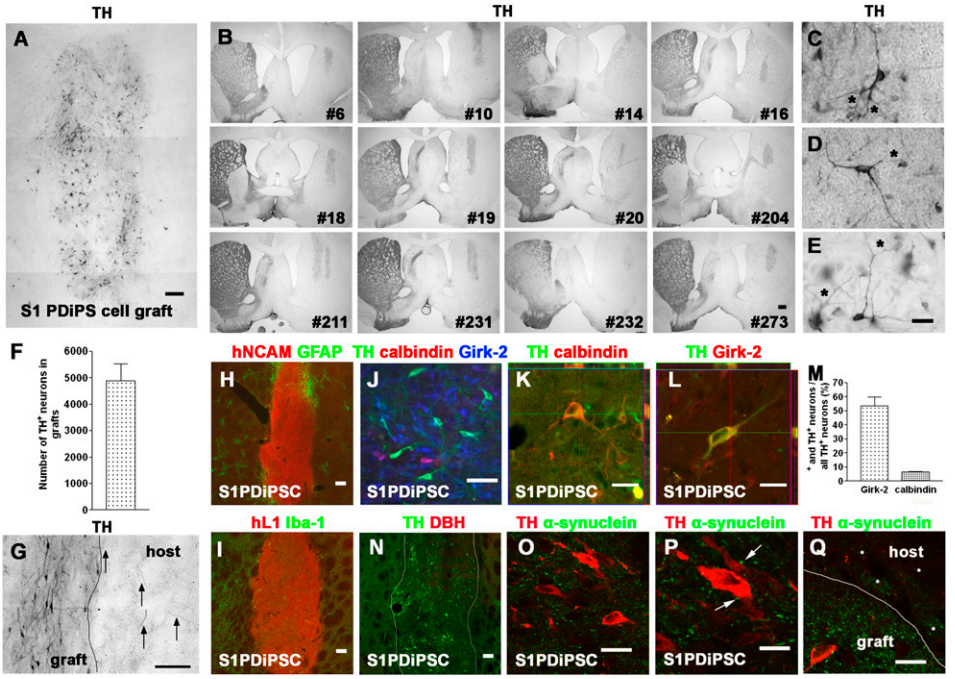

Fig. 3. PDiPS cell-derived DA neurons survive at high numbers after transplantation into the striatum of 6-OHDA–lesioned rats. (*A–E* and *G*) Photomicrographs of engrafted differentiated S1 PDiPS cells immunostained for TH 16 wk after transplantation of 400,000 cells into 6-OHDA–lesioned rats. (*A*) TH$^+$ DA neurons were present at high numbers throughout the PDiPS cell grafts. Three images were assembled for graft reconstruction. (*B*) Low-power photomicrographs show that all 12 transplanted rats contained TH$^+$ grafts in the DA-depleted striatum. Numbers indicate individual rats. (*C–E*) DA neurons with fiber arborization and branching (asterisks) in grafts. (*F*) Quantification of DA neurons in PDiPS cell grafts. (*G*) Some graft-derived TH$^+$ fibers (arrows) project into the host lesioned striatum. (*H*) Immunostainings of grafts for hNCAM (red) and GFAP (green) and (*I*) for hL1 (red) and Iba-1 (green) show low astroglial and microglial reaction around the grafts. (*N*) Immunostaining of engrafted cells for TH (green) and DBH (red) showing DA, although not noradrenergic, neurons in grafts. (*J–M*) Girk-2 and calbindin were expressed in engrafted DA neurons. (*J*) Immunostaining of engrafted cells for TH (green), calbindin (red), and Girk-2 (blue). (*K* and *L*) Z-stacks of three confocal images show coexpression of (*K*) TH (green) and calbindin (red) or (L) TH (green) and Girk-2 (red) in engrafted DA neurons. (*M*) Quantification of stainings for TH, calbindin, and Girk-2 in PDiPS cell grafts. (*O–Q*) Immunostainings for TH (red) and α-synuclein (green; human-specific antibody) show a punctate synaptic expression of α-synuclein on engrafted TH$^+$ neurons (arrows, *P*) and in the host striatum (asterisks, *Q*). (Scale bars: 10 μm in *P*; 20 μm in *K*, *L*, *O*, and *Q*; 25 μm in *C–E*; 50 μm in *J*; 100 μm in *A*, *G*, *H*, *I*, and *N*; 500 μm in *B*.)

tations up to 16 wk after transplantation (Fig. 4 *A–C*). The number of rotations was significantly lower compared with the control group at this time point (Fig. 4*A*). Nine of 12 animals showed a significant reduction in amphetamine-induced rotations at 16 wk after transplantation (Fig. 4 *B* and *C*). The apomorphine-induced rotation test evaluates the effect of engrafted DA neurons on 6-OHDA–induced hypersensitivity of striatal DA receptors. We found that transplanted rats showed a significantly reduced number of contralateral rotations 16 wk after engraftment compared with the control group (Fig. 4*D*). The cylinder test and the adjustment stepping test evaluate the connectivity of engrafted DA neurons with host striatal neurons, which control complex motor functions. Consistent with our findings on the limited outgrowth of implanted DA neurons, we did not detect an improved performance in either of these tests in the PDiPS cell-transplanted group compared with the control group at 16 wk after transplantation (Fig. S3).

We next applied FACS for NCAM on differentiated S1 and FF21-26 PDiPS cells before transplantation to further reduce the risk of tumor formation and to examine if the sorted DA neurons would survive in adult rodent brain (Fig. 4 *E–G* and Fig. S4). Five lesioned rats were transplanted with sorted PDiPS cells and grafts were analyzed at 8 wk ($n = 1$) and 16 wk ($n = 4$) after transplantation. The sorted PDiPS cell grafts were positive for hNCAM and hL1, and none of the grafts showed signs of tumor formation (Fig. 4*E* and Fig. S4). In all grafts, surviving DA neurons were found at a mean number of 344 ± 92 DA neurons per graft. Probably because of relatively small graft sizes and limited axonal outgrowth, effects on apomorphine-induced rotational asymmetry were not significant and were observed in only one animal 16 wk after transplantation (Fig. S4). However, all animals transplanted with sorted PDiPS cells showed a significant reduction of amphetamine-induced rotations at 16 wk after transplantation compared with control animals ($n = 5$), which did not improve over time (Fig. 4*G* and Fig. S4).

Discussion

The application of patient-derived iPS cells for cell therapy has the advantage of using genetically identical cells, which can be introduced into a patient without the need for immunosuppression. Here, we differentiated iPS cell lines from three patients with sporadic PD into DA neurons and applied a series of in vivo experiments on these cells. We used cell transplantation as a long-term in vivo bioassay on PDiPS cells, which provides opportunities to study cell development, neuronal maturation, and neuronal cell survival, and importantly, allows evaluation of potential degenerative changes in a physiological 3D context over a prolonged time period. In all PDiPS cell groups, we found viable grafts for at least 12 wk after transplantation that stained positive for hNCAM and hL1. None of the PDiPS cell-derived neurons showed signs of inclusion body formation or other morphological features that would indicate a neurodegenerative process in the cells. An analysis of the axonal outgrowth of engrafted neurons derived from PDiPS cells, non-PDiPS cells, and hES cells revealed a specific and reproducible pattern, which was highly conserved within and between groups. These data show that permissive guidance cues for developing axons are still present in the adult rodent brain, and that the implanted human iPS and ES cell-derived

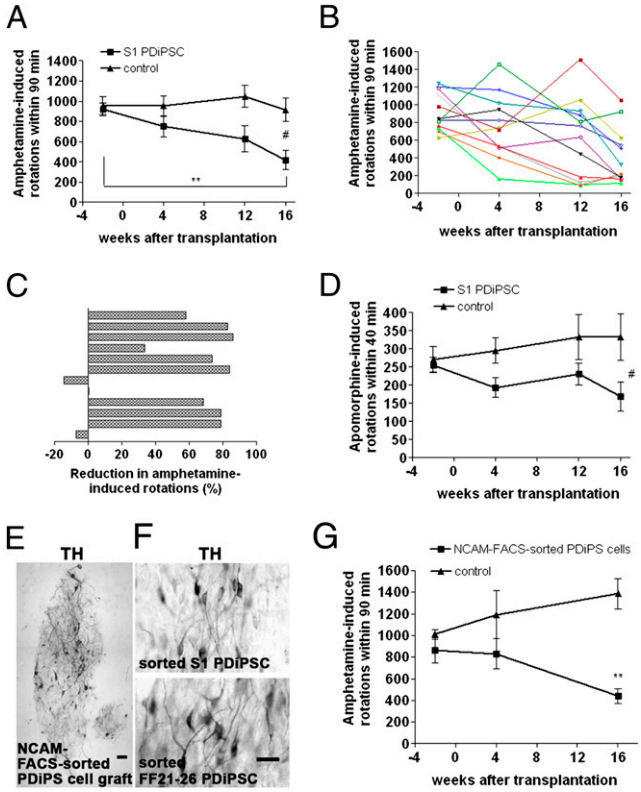

Fig. 4. Reduced motor asymmetry of 6-OHDA–lesioned rats after intrastriatal transplantation of differentiated PDiPS cells. (*A–C*) Amphetamine-induced rotations of S1 PDiPS cell–transplanted rats (n = 12) significantly declined over time (**$P < 0.01$) and were significantly less compared with control rats (n = 9) 16 wk after transplantation ($^{\#}P < 0.05$). (*B*) Number of rotations of each rat over time. (*C*) The percentage of the reduction in rotations 16 wk after transplantation. (*D*) Apomorphine-induced rotations of rats over time reveal a significantly decreased number of rotations in PDiPS cell–treated rats 16 wk after transplantation compared with control rats ($^{\#}P < 0.05$). (*E–G*) Differentiated S1 and FF21-26 PDiPS cells were FACS-sorted for NCAM and subsequently engrafted into five 6-OHDA–lesioned rats (S1, n = 2; FF21-26, n = 3). (*E* and *F*) Photomicrographs of TH$^+$ DA neurons 16 wk after transplantation. Three images were assembled in panel E for graft reconstruction. (Scale bars: 50 μm in *E*; 25 μm in *F*.) (*G*) The number of amphetamine-induced rotations of rats engrafted with sorted PDiPS cells was significantly lower compared with control rats (n = 5) 16 wk after transplantation (**$P < 0.01$). Graphs show mean values ± SEM. Two-way ANOVA with post hoc Tukey test was performed for statistical analysis.

neurons were responsive to these guidance cues independent of the ES or PD donor cell origin. It has previously been demonstrated in xenografting experiments that engrafted donor neurons project to their target areas according to their intrinsic phenotypic determination (19–21). In this study, several brain areas were specifically innervated by implanted cells, which indicates that different neuronal phenotypes, including cortical projection neurons, had survived in the grafts. Although we could not detect PD-related changes in axonal fiber outgrowth, other parameters such as axonal transport, synaptogenesis, synaptic pruning, or synaptic function could be further analyzed for PD-related changes by applying such an in vivo bioassay. In addition, observation periods could be further prolonged for up to 2 to 3 y to evaluate any disease-related changes, which might occur outside the time window described in this study, and other host models including SCID mice (22) could be considered, which do not require the application of immunosuppressive agents.

The initial transplantation experiments in this study showed that DA neurons survived in all unlesioned animals of the PDiPS cell groups for many months after transplantation. We therefore transplanted differentiated PDiPS cells into the striatum of 6-OHDA–lesioned rats as a functional and behavioral model for PD. In all animals, viable grafts with a high number of DA neurons without signs of neurodegeneration were found 16 wk after transplantation, and the survival rate of these DA neurons—an indirect measure for cell vulnerability—was comparable to those shown in studies on engrafted differentiated hES cells (13) or primate ES cells (23) 16 to 20 wk after transplantation. The PDiPS cell-derived DA neurons showed functional effects as demonstrated by a significant reduction in amphetamine- and apomorphine-induced rotations 16 wk after transplantation. Nine of 12 animals showed a significant reduction in amphetamine-induced asymmetry and the degree of behavioral improvement reached more than 70% in the majority of these rats. One rat without improvement had a misplaced graft that reached into the globus pallidum, and another rat presented with an unusually wide ventricular system. Although the reduction of motor asymmetry was prominent, a full recovery was not observed up to 16 wk after transplantation. This is possibly because of the long maturation process that human DA neurons have to undergo in vivo, as reported in studies on implanted human mesencephalic DA neurons that show a significant reduction in amphetamine-induced rotation at 15 wk, but only full recovery by 20 wk after transplantation (24). Given that the transplanted rats improved gradually over time, more pronounced effects might have occurred if the rats had been analyzed for a longer period after transplantation. We did not detect any effects in cylinder and adjustment stepping tests, which is probably a result of the observed poor outgrowth of implanted PDiPS cells to host neurons in the striatum. Reduced outgrowth of DA neurons has previously been described for both implanted differentiated mouse (25) and human (13) ES cells and is therefore unlikely to be PD- or iPS cell–related. This is supported by the fact that we could not detect PD- or iPS cell–related differences in axonal outgrowth of engrafted neurons in our in vivo bioassays. Increasing the number of cells for transplantation and further improvements of the differentiation protocol might lead to better functional outcomes. Approximately 50% of the engrafted PDiPS cell-derived DA neurons coexpressed Girk-2, which, together with TH, is typically expressed in substantia nigra (A9) DA neurons that project into striatal tissue. However, only a few graft-derived DA axons were found to innervate the host striatum, indicating a heterogenous population of engrafted Girk-2- and TH-coexpressing DA neurons. Indeed, a subset of other neurons outside the A9 region also coexpress TH and Girk-2 (26) and the engrafted PDiPS cell-derived DA neurons did not coexpress the transcription factor foxA2 that is found together with TH in most A9 midbrain DA neurons (27). Therefore, we believe the PDiPS cells have most likely been inefficiently patterned toward an A9 DA neuronal phenotype during in vitro differentiation. Notably, hES cell-derived DA neurons also have not yet been shown to coexpress TH and foxA2 after transplantation using different differentiation protocols, including ours (12–15), indicating that new strategies toward phenotypic patterning of hES and hiPSs cells during in vitro differentiation have to be pursued. During the course of this study, however, we and others have developed protocols that generate foxA2$^+$ floor plate cells from hES cells (28) or foxA2$^+$ DA neurons from hES and PDiPS cells in vitro (29), which provide encouraging cell sources for future transplantation studies to further improve axonal outgrowth and behavioral outcomes.

None of the 48 PDiPS cell grafts analyzed in this study showed signs of tumor formation up to 16 wk after transplantation. However, we and others have previously shown that tumor formation can occur when transplanting human pluripotent stem cell-derived cells (14, 15), demonstrating a requirement to further purify cells before transplantation. Therefore, we performed FACS of differentiated PDiPS cells for NCAM before transplantation and

did not observe signs of tumor formation in the grafts. Instead, NCAM-purified DA neurons had survived in all grafts, which also showed functional effects on amphetamine-induced rotational asymmetry. Interestingly, engrafted factor-carrying PDiPS cells did not express oct4 at 16 wk after transplantation. Oct4 is one of the factors used during derivation of PDiPS cells (7) indicating that sufficient gene silencing is possible in engrafted iPS cells. However, factor-free PDiPS cells constitute a safer cell source for cell replacement approaches, and therefore we have characterized these cells along with factor-carrying PDiPS cells in this study. Future clinical applications will likely demand new techniques for generating factor-free iPS cells such as virus-free (30) or DNA-free approaches (31) at acceptable efficiencies.

The present study provides a basis for future comparative studies on iPS cell lines from patients with genetic PD (genPDiPS cells). Mutations in the PD-related genes LRRK2 or α-synuclein have been linked to an impairment of neurite outgrowth (32, 33) that, together with potential inclusion body formation or potential changes in DA cell survival, could be evaluated in a physiological context in long-term in vivo bioassays as described here. Such in vivo bioassays can be further applied to analyze function of genPDiPS cells in vivo, to test new drugs on engrafted genPDiPS cells, or to validate any in vitro gene targeting approaches that might be necessary in genPDiPS cells before they can be considered for applications in vivo. Importantly, the present study provides a proof of principle that engrafted PDiPS cells can have functional effects in an animal model of PD. At the same time, it encourages to further improve differentiation protocols and cell purification methods, as well as strategies to generate patient-specific iPS cells for future clinical applications.

Methods

In Vitro Differentiation of Human Stem Cells. Human stem cells were maintained on mitomycin C–inactivated human D551 fibroblasts (American Type Culture Collection) and were differentiated according to a stromal feeder cell–based protocol (18), which was modified through the addition of noggin (300 ng/mL) during the first 21 d of differentiation to improve neuroectodermal differentiation (14).

Cell Transplantation and Behavioral Analysis. All animal procedures were performed according to National Institutes of Health guidelines and were approved by the Institutional Animal Care and Use Committee at McLean Hospital and Harvard Medical School. Differentiated cells were harvested at day 42 in vitro and transplanted into the striatum of adult Sprague-Dawley rats at a density of 100,000 viable cells per microliter. The surgical procedures and behavioral tests have been described in detail (14, 23). Amphetamine and apomorphine were applied at doses of 4 mg/kg i.p. or 0.1 mg/kg s.c., respectively. Data were analyzed using Statistica software (StatSoft).

Immunohistochemistry and Cell Counts. Immunostainings of brain sections were performed as previously described (14, 23). Cell counts of DA neurons in 6-OHDA–lesioned rats were obtained by applying the fractionator probe. Only TH^+ cells with visible neurites were counted. A detailed description of all methods can be found in *SI Methods*.

ACKNOWLEDGMENTS. We thank Andrew Kartunen for excellent technical help. This study was supported by the Udall Parkinson's Disease Center of Excellence Grant P50 NS39793 (to O.I.), Michael Stern Foundation Grant WX81XWH-05-1-0555 (to O.I.), Parkinson's Disease iPS Cell Line Research Consortium Grant 1RC2NS070276-01 (to O.I.), Orchard Foundation (O.I.), the Consolidated Anti-Aging Foundation (O.I.), Harold and Ronna Cooper Family (O.I.); National Institutes of Health Grants R01-HD045022 (to R.J.) and R01 CA098959-01 (to R.J.), a Collaborative Innovation Award from the Howard Hughes Medical Institute (R.J.), postdoctoral fellowship HA5589/1-1 from the Deutsche Forschungsgemeinschaft (to G.H.), and Training Award T32AG000222-17 from the National Institute on Aging (to T.O.). D.H. is a Merck Fellow of the Life Science Research Foundation.

1. Takahashi K, Yamanaka S (2006) Induction of pluripotent stem cells from mouse embryonic and adult fibroblast cultures by defined factors. *Cell* 126:663–676.
2. Saha K, Jaenisch R (2009) Technical challenges in using human induced pluripotent stem cells to model disease. *Cell Stem Cell* 5:584–595.
3. Wernig M, et al. (2008) Neurons derived from reprogrammed fibroblasts functionally integrate into the fetal brain and improve symptoms of rats with Parkinson's disease. *Proc Natl Acad Sci USA* 105:5856–5861.
4. Raya A, et al. (2009) Disease-corrected haematopoietic progenitors from Fanconi anaemia induced pluripotent stem cells. *Nature* 460:53–59.
5. Park IH, et al. (2008) Disease-specific induced pluripotent stem cells. *Cell* 134:877–886.
6. Maehr R, et al. (2009) Generation of pluripotent stem cells from patients with type 1 diabetes. *Proc Natl Acad Sci USA* 106:15768–15773.
7. Soldner F, et al. (2009) Parkinson's disease patient-derived induced pluripotent stem cells free of viral reprogramming factors. *Cell* 136:964–977.
8. Ebert AD, et al. (2009) Induced pluripotent stem cells from a spinal muscular atrophy patient. *Nature* 457:277–280.
9. Lee G, et al. (2009) Modelling pathogenesis and treatment of familial dysautonomia using patient-specific iPSCs. *Nature* 461:402–406.
10. Astradsson A, Cooper O, Vinuela A, Isacson O (2008) Recent advances in cell-based therapy for Parkinson disease. *Neurosurg Focus* 24:E6.
11. Lindvall O, Kokaia Z (2009) Prospects of stem cell therapy for replacing dopamine neurons in Parkinson's disease. *Trends Pharmacol Sci* 30:260–267.
12. Ben-Hur T, et al. (2004) Transplantation of human embryonic stem cell-derived neural progenitors improves behavioral deficit in Parkinsonian rats. *Stem Cells* 22:1246–1255.
13. Yang D, Zhang ZJ, Oldenburg M, Ayala M, Zhang SC (2008) Human embryonic stem cell-derived dopaminergic neurons reverse functional deficit in parkinsonian rats. *Stem Cells* 26:55–63.
14. Sonntag KC, et al. (2007) Enhanced yield of neuroepithelial precursors and midbrain-like dopaminergic neurons from human embryonic stem cells using the bone morphogenic protein antagonist noggin. *Stem Cells* 25:411–418.
15. Roy NS, et al. (2006) Functional engraftment of human ES cell-derived dopaminergic neurons enriched by coculture with telomerase-immortalized midbrain astrocytes. *Nat Med* 12:1259–1268.
16. Pruszak J, Sonntag KC, Aung MH, Sanchez-Pernaute R, Isacson O (2007) Markers and methods for cell sorting of human embryonic stem cell-derived neural cell populations. *Stem Cells* 25:2257–2268.
17. Pruszak J, Ludwig W, Blak A, Alavian K, Isacson O (2009) CD15, CD24, and CD29 define a surface biomarker code for neural lineage differentiation of stem cells. *Stem Cells* 27:2928–2940.
18. Perrier AL, et al. (2004) Derivation of midbrain dopamine neurons from human embryonic stem cells. *Proc Natl Acad Sci USA* 101:12543–12548.
19. Wictorin K, Brundin P, Gustavii B, Lindvall O, Björklund A (1990) Reformation of long axon pathways in adult rat central nervous system by human forebrain neuroblasts. *Nature* 347:556–558.
20. Isacson O, et al. (1995) Transplanted xenogeneic neural cells in neurodegenerative disease models exhibit remarkable axonal target specificity and distinct growth patterns of glial and axonal fibres. *Nat Med* 1:1189–1194.
21. Isacson O, Deacon TW (1996) Specific axon guidance factors persist in the adult brain as demonstrated by pig neuroblasts transplanted to the rat. *Neuroscience* 75:827–837.
22. Shultz LD, Ishikawa F, Greiner DL (2007) Humanized mice in translational biomedical research. *Nat Rev Immunol* 7:118–130.
23. Sanchez-Pernaute R, et al. (2008) Parthenogenetic dopamine neurons from primate embryonic stem cells restore function in experimental Parkinson's disease. *Brain* 131:2127–2139.
24. Brundin P, et al. (1986) Behavioural effects of human fetal dopamine neurons grafted in a rat model of Parkinson's disease. *Exp Brain Res* 65:235–240.
25. Yurek DM, Fletcher-Turner A (2004) Comparison of embryonic stem cell-derived dopamine neuron grafts and fetal ventral mesencephalic tissue grafts: morphology and function. *Cell Transplant* 13:295–306.
26. Schein JC, Hunter DD, Roffler-Tarlov S (1998) Girk2 expression in the ventral midbrain, cerebellum, and olfactory bulb and its relationship to the murine mutation weaver. *Dev Biol* 204:432–450.
27. Ferri AL, et al. (2007) Foxa1 and Foxa2 regulate multiple phases of midbrain dopaminergic neuron development in a dosage-dependent manner. *Development* 134:2761–2769.
28. Fasano CA, Chambers SM, Lee G, Tomishima MJ, Studer L (2010) Efficient derivation of functional floor plate tissue from human embryonic stem cells. *Cell Stem Cell* 6:336–347.
29. Cooper O, et al. (2010) Differentiation of human ES and Parkinson's disease iPS cells into ventral midbrain dopaminergic neurons requires a high activity form of SHH, FGF8a and specific regionalization by retinoic acid. *Mol Cell Neurosci*, Jul 23 [published ahead of print].
30. Yu J, et al. (2009) Human induced pluripotent stem cells free of vector and transgene sequences. *Science* 324:797–801.
31. Kim D, et al. (2009) Generation of human induced pluripotent stem cells by direct delivery of reprogramming proteins. *Cell Stem Cell* 4:472–476.
32. MacLeod D, et al. (2006) The familial Parkinsonism gene LRRK2 regulates neurite process morphology. *Neuron* 52:587–593.
33. Marongiu R, et al. (2009) Mutant Pink1 induces mitochondrial dysfunction in a neuronal cell model of Parkinson's disease by disturbing calcium flux. *J Neurochem* 108:1561–1574.

Supporting Information

Hargus et al. 10.1073/pnas.1010209107

SI Methods

Culture and in Vitro Differentiation of Human Stem Cells. The human ES cell line H9 (National Institutes of Health code WA09; Wisconsin Alumni Research Foundation, Madison, WI), a non-PDiPS cell line, and four PDiPS cell lines (1) were maintained on mitomycin C–inactivated human fibroblasts (D551; American Type Culture Collection) and were mechanically passaged every 6 to 8 d. All experiments with human ES cells were approved by the Partners Embryonic Stem Cell Research Oversight (ESCRO) Committee under protocol number 2006-04-001A. For differentiation, a stromal feeder cell-based protocol (2) was used that was modified to improve neuroectodermal differentiation (3) (Fig. S1). Stem cells were cultured on mitomycin C– inactivated MS5-Wnt1 stromal feeder cells for 14 d in serum replacement medium (KnockOut DMEM supplemented with 15% KnockOut Serum Replacement, 1mM glutamine, and 1% nonessential amino acids; all from Invitrogen), followed by 7 d of culture in N2 medium consisting of DMEM/F12 (Invitrogen) supplemented with N2-A (Stem Cell Technologies). During these first 21 d of culture, 300 ng/mL noggin (R&D Systems) was added to the media. Neural rosettes were mechanically isolated at d 21 of differentiation and subsequently plated on poly L-ornithine- (15 μg/mL; Sigma-Aldrich) and laminin- (1 μg/mL; Sigma-Aldrich) coated culture dishes. DA differentiation was favored by culturing cells for 16 d in N2 medium containing 200 ng/mL N-terminal fragment of Shh (R&D Systems), 100 ng/mL murine FGF8 isoform b (R&D Systems), 20 ng/mL BDNF (PeproTech), and 200 μM ascorbic acid (Sigma-Aldrich). Cells terminally differentiated into mature DA neurons in N2-medium containing 20 ng/mL BDNF, 1 ng/mL TGF-β3 (Calbiochem), 10 ng/mL GDNF (Sigma-Aldrich), 0.5 mM dibutyryl cAMP (Sigma-Aldrich), and 200 μM ascorbic acid for 5 d.

Transplantation of Differentiated Human Stem Cells. All animal procedures were performed according to National Institutes of Health guidelines and were approved by the Institutional Animal Care and Use Committee at McLean Hospital and Harvard Medical School. Adult female Sprague-Dawley rats (200–250 g) were purchased from Charles River. In addition, female Sprague-Dawley rats with a unilateral 6-OHDA lesion were obtained from Taconic Farms. A maximum of four animals per cage were housed under standard conditions in the animal facility at McLean Hospital. Human stem cells were differentiated and harvested at day 42 in vitro. Cells were gently dissociated by 0.05% trypsin/EDTA (Invitrogen) and resuspended in cold HBSS (Invitrogen) supplemented with 4.5 mg/mL sucrose (Sigma-Aldrich) and 1 μg/mL GDNF (Sigma-Aldrich) at a density of 100,000 viable cells per microliter. Unlesioned rats received 200,000 cells as a single deposit at the following coordinates from bregma (site 1): anteroposterior, +0.4; mediolateral, −3.0; dorsoventral, −5.0. Lesioned rats received 400,000 cells as two deposits of 200,000 cells using the same coordinates (site 1) and the following coordinates from bregma (site 2): anteroposterior, −0.5; mediolateral, −3.6; dorsoventral, −5.0. The same coordinates (sites 1 and 2) were used for the transplantation of approximately 200,000 to 400,000 NCAM-FACS-sorted PDiPS cells. The staining of differentiated human pluripotent stem cells with an NCAM antibody (Santa Cruz Biotechnology) and the FACS sorting procedure have been previously described (4). Cells were carefully engrafted at a rate of 0.3 μL/min. The numbers of unlesioned rats studied were as follows: H9 hES cells (n = 4), A6 non-PDiPS cells (n = 4), K1 PDiPS cells (n = 14), S1 PDiPS cells (n = 6), FF17-5 PDiPS cells (n = 7), and FF21-26 PDiPS cells (n = 9). For functional analysis, twelve 6-OHDA–lesioned rats were engrafted with differentiated S1 PDiPS cells and five 6-OHDA rats received differentiated NCAM-FACS–sorted S1 (n = 2) or FF21-26 (n = 3) PDiPS cells. One day before surgery, the rats were injected with 30 mg/kg cyclosporine A (Sandimmune; Sandoz), and rats received 15 mg/kg cyclosporine A daily starting from the day of surgery to prevent graft rejection.

Behavioral Tests. Two weeks before transplantation, rotational asymmetry of 6-OHDA–lesioned rats was analyzed after i.p. injection of amphetamine (4 mg/kg; 90 min) or s.c. injection of apomorphine (0.1 mg/kg; 40 min), respectively. Functionally lesioned rats were randomly assigned to two groups, one control group (n = 9) and one group for the transplantation of differentiated S1 PDiPS cells (n = 12). Amphetamine- and apomorphine-induced rotations were evaluated at 4, 8, 12, and 16 wk after transplantation. For the FACS experiments, five control animals and five stem cell–treated 6-OHDA–lesioned rats were analyzed. To test the spontaneous use of forelimbs, a cylinder test was applied on the rats 2 wk before and 16 wk after transplantation. Rats were videotaped in a plastic cylinder for 2 min in the light and 2 min in the dark. The number of contacts on the wall during rearing was counted for each paw. The data are presented as left paw contacts over right paw contacts. An adjustment stepping test was performed on the rats 16 wk after transplantation as previously described (5). The hindlimbs and one forelimb were fixed by the experimenter and the rats were moved sideways along a flat surface (0.9 m in 5 s) to assess the number adjusting steps performed by the free forelimb. This test was repeated four times per side and rat. Average values were taken for comparative analysis.

Immunocytochemistry and Immunohistochemistry. Cultured cells were fixed in 4% paraformaldehyde and incubated in 10% normal goat or donkey serum for 1 h at room temperature. Primary antibodies were added for 3 h at room temperature followed by incubation with appropriate secondary antibodies for 1 h. For immunohistochemistry, animals were intracardially perfused with heparinized saline solution (0.1% heparin in 0.9% saline solution) and 4% paraformaldehyde (pH 7.4) 4, 8, 12, or 16 wk after transplantation after receiving an i.p. overdose of pentobarbital (150 mg/kg). Perfused brains were soaked in 30% sucrose and were sectioned on a microtome in 40-μm slices, which were serially collected. Primary antibodies were used at room temperature overnight and are listed in Table S2. Appropriate fluorescence-labeled secondary antibodies (Alexa Fluor; Invitrogen) were used and nuclei were stained with Hoechst 33342 (5 μg/mL; Sigma-Aldrich). For light microscopy, biotinylated secondary antibodies (1:300; Vector Laboratories) were applied to detect anti-TH or anti-hNCAM antibodies, followed by incubation in streptavidin–biotin complex (Vectastain ABC Kit Elite; Vector Laboratories) for 1 h and visualized by incubation in 3,3′-diaminobenzidine (Vector Laboratories).

Evaluation of Fiber Outgrowth and Stereological Analysis. Engrafted human stem cell–derived neurons were visualized using a human-specific antibody directed against NCAM. The fiber outgrowth of engrafted neurons was followed throughout the brain and the number of axons per target area was evaluated in sections of 40-μm thickness. A StereoInvestigator software-controlled computer system (MicroBrightField) and an Axioskop microscope (Carl Zeiss) were used for quantitative analysis of graft volume, numbers of engrafted cells, and cellular phenotypes in vitro. For immunocytochemical analysis, cells in randomly selected visual fields

from at least three separate differentiation experiments were counted. At least 3,000 Hoechst-positive cells per experiment were analyzed for expression of TH and β III-tubulin in a blinded manner. Unbiased estimates of the volume of transplants were calculated using the Cavalieri estimator probe on hNCAM-stained serial brain sections. Cell counts were obtained applying the fractionator probe. Every fifth 40-μm-thick section of the graft was analyzed and only TH^+ cells with visible neurites were counted. Confocal analysis using an LSM510 Meta confocal microscope (Carl Zeiss) was performed to assess colocalization of marker molecules in engrafted cells, keeping optical sections to a minimal thickness. To evaluate the percentage of marker-coexpressing cells within the grafts, random sampling in graft core and periphery was performed at 40× magnification. Three-dimensional reconstructions of stacked z-images of 1 μm thickness with orthogonal views of the *xz*- and *yz*-planes were obtained using LSM Examiner software (Carl Zeiss).

1. Soldner F, et al. (2009) Parkinson's disease patient-derived induced pluripotent stem cells free of viral reprogramming factors. *Cell* 136:964–977.
2. Perrier AL, et al. (2004) Derivation of midbrain dopamine neurons from human embryonic stem cells. *Proc Natl Acad Sci USA* 101:12543–12548.
3. Sonntag KC, et al. (2007) Enhanced yield of neuroepithelial precursors and midbrain-like dopaminergic neurons from human embryonic stem cells using the bone morphogenic protein antagonist noggin. *Stem Cells* 25:411–418.
4. Pruszak J, Sonntag KC, Aung MH, Sanchez-Pernaute R, Isacson O (2007) Markers and methods for cell sorting of human embryonic stem cell-derived neural cell populations. *Stem Cells* 25:2257–2268.
5. Olsson M, Nikkhah G, Bentlage C, Björklund A (1995) Forelimb akinesia in the rat Parkinson model: Differential effects of dopamine agonists and nigral transplants as assessed by a new stepping test. *J Neurosci* 15:3863–3875.

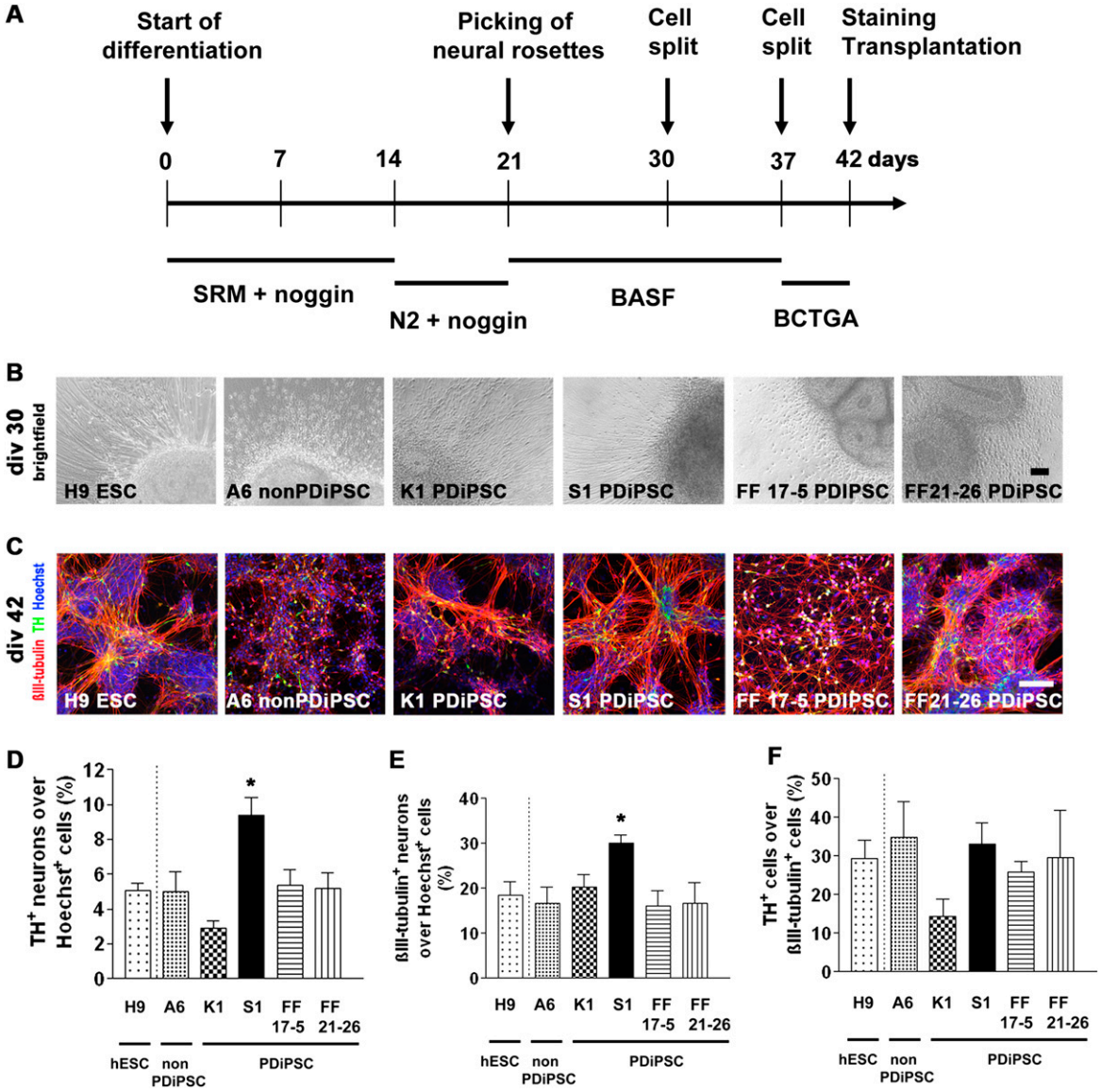

Fig. S1. PDiPS cells differentiate into dopaminergic neurons in vitro. (*A*) Scheme shows the timeline and factors used to differentiate hES cells, non-PDiPS cells, and PDiPS cells into DA neurons in vitro (according to refs. 1, 2). (*B*) Bright-field images showing that all cell lines differentiated into neural rosettes in vitro. (Scale bar: 100 μm.) (*C*) Immunofluorescence stainings of differentiated cells for TH (green), β III-tubulin (red), and Hoechst (blue). All cell lines differentiated into DA neurons in vitro. (Scale bar: 100 μm.) (*D–F*) Quantifications of immunostainings for TH and β III-tubulin at day 42 in vitro. The S1 PDiPS cell line showed enhanced neuronal, although not DA, differentiation. All graphs show mean values + SEM. One-way ANOVA with Dunnett multiple comparison test was performed for statistical analysis (*$P < 0.05$). SRM: serum replacement medium; BASF: BDNF, ascorbic acid, sonic hedgehog, and FGF-8b; BCTGA: BDNF, cyclic AMP, TGF-β, GDNF, and ascorbic acid.

1. Sonntag KC, et al. (2007) Enhanced yield of neuroepithelial precursors and midbrain-like dopaminergic neurons from human embryonic stem cells using the bone morphogenic protein antagonist noggin. *Stem Cells* 25:411–418.
2. Perrier AL, et al. (2004) Derivation of midbrain dopamine neurons from human embryonic stem cells. *Proc Natl Acad Sci USA* 101:12543–12548.

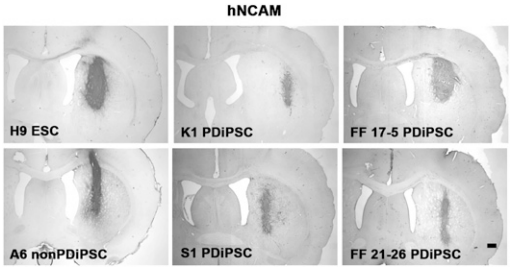

Fig. S2. Engrafted PDiPS cell-, non-PDiPS cell–, and hES cell-derived neurons send out fibers to the surrounding gray and white matter in the adult unlesioned rodent brain. Photomicrographs of hNCAM-stained brain sections with grafts consisting of differentiated H9 hES cells, A6 non-PDiPS cells, and the four differentiated PDiPS cell lines K1, S1, FF 17–5, and FF 21–26 at 4 wk after transplantation. All grafts contained a high number of hNCAM$^+$ cells, which sent projections to the surrounding gray and white matter. (Scale bar: 500 μm.)

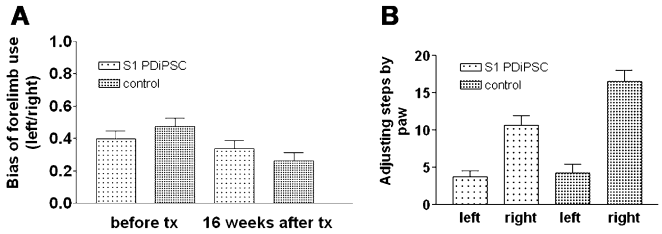

Fig. S3. Cylinder and adjustment stepping tests of 6-OHDA–lesioned rats after intrastriatal transplantation of differentiated PDiPS cells. (*A*) A cylinder test and (*B*) an adjustment stepping test were performed on PDiPS cell-transplanted and nontransplanted control rats at 16 wk after transplantation. Both tests did not show differences between the groups. The graphs show mean values + SEM.

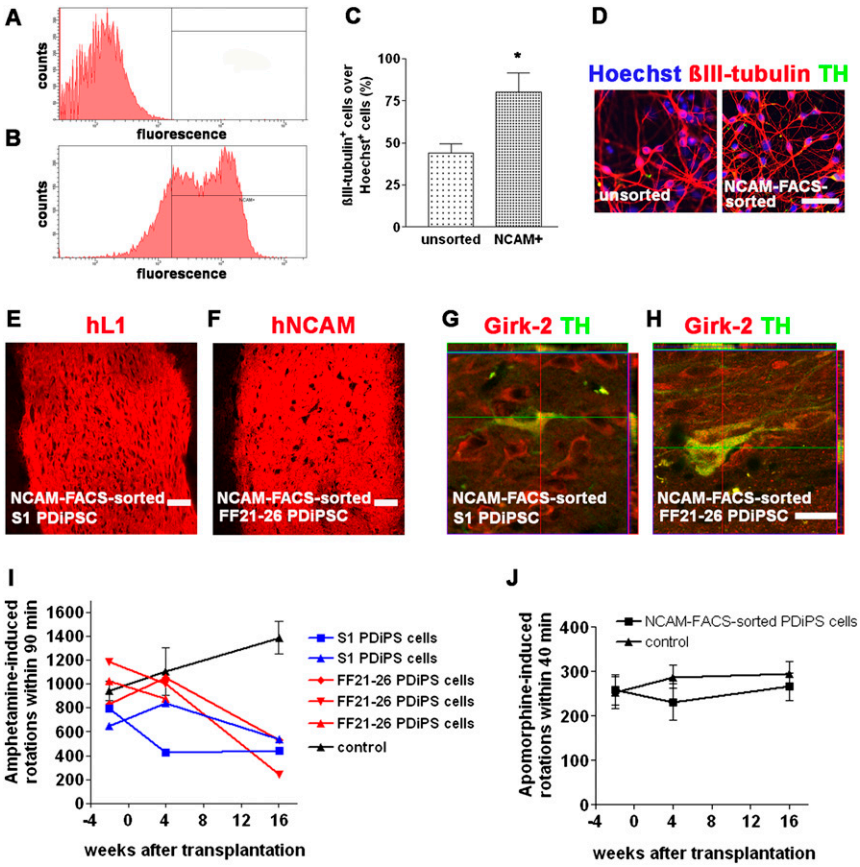

Fig. S4. NCAM-FACS–sorted PDiPS cells survive after transplantation into 6-OHDA–lesioned rats. Differentiated PDiPS cells were FACS-sorted for NCAM at day 42 in vitro. FACS plots show isotype control (*A*) and the NCAM$^+$ fraction (*B*). (*C*) NCAM-FACS–sorted cells were replated and counted 1 d after sorting. Results from three independent experiments are shown and demonstrate an enrichment in neuronal cells after sorting. (*D*) Immunofluorescence staining of unsorted and NCAM-FACS-sorted differentiated PDiPS cells for β III-tubulin (red), TH (green), and Hoechst (blue) 3 d after replating. (*E–J*) Differentiated S1 and FF21-26 PDiPS cells were sorted for NCAM and were transplanted into the striatum of five 6-OHDA–lesioned rats (S1, $n = 2$; FF21-26, $n = 3$). Immunostainings for hL1 (*E*) and hNCAM (*F*) show neuronal PDiPS cell grafts 16 wk after NCAM sorting and transplantation. (*G* and *H*) Z-stacks of three confocal images of 1 μm thickness show coexpression of TH (green) and Girk-2 (red) in engrafted NCAM-FACS–sorted S1 and FF21-26 PDiPS cell-derived DA neurons. (*I*) Amphetamine-induced rotations of rats transplanted with NCAM-FACS-sorted PDiPS cells were significantly less compared with nontransplanted control rats ($n = 5$) 16 wk after transplantation. The numbers of amphetamine-induced rotations over time are shown for each rat. (*J*) Apomorphine-induced rotations of nontransplanted control rats and of rats with sorted PDiPS cells did not show a difference over time. Student's *t* test was used for statistical analysis in *C* (*$P < 0.05$).

Table S1. Target areas and densities of engrafted human ES cell-, non-PDiPS cell–, and PDiPS cell-derived hNCAM-positive axons in the adult rodent brain

Area	Score					
	H9 ES cells	A6 non-PDiPS cells	K1 PDiPS cells	S1 PDiPS cells	FF 17–5 PDiPS cells	FF 21–26 PDiPS cells
Telencephalic cortical targets						
Ipsilateral cortex (general)	4	4	4	4	4	4
Ipsilateral cingulate cortex	2	1	2	1	2	2
Ipsilateral frontal/sec motor cortex	4	4	4	4	4	4
Ipsilateral somatosensory cortex	4	3	3	4	2	2
Ipsilateral insular cortex	4	4	4	4	2	2
Ipsilateral piriform cortex	4	4	4	4	3	3
Ipsilateral dorsal endopiriform cortex	3	3	3	4	3	3
Contralateral cortex (general)	3	2	3	3	2	2
Contralateral frontal/sec motor cortex	3	2	2	2	1	1
Contralateral somatosensory cortex	2	1	2	2	1	2
Basal ganglia and nuclei						
Caudate putamen	4	4	4	4	4	4
Contralateral caudate putamen	0	0	0	0	0	0
External globus pallidum	4	4	4	4	4	4
Internal globus pallidum	4	4	4	4	4	4
Basal nucleus of Meynert	4	4	4	4	4	4
Lateral septal nucleus	4	4	4	4	4	4
Claustrum	4	4	4	4	4	4
Ventral pallidum	4	4	4	4	4	4
Accumbens nucleus	4	4	4	4	3	4
Central amygdala nucleus	4	4	1	4	3	4
Subthalamic nucleus	4	4	4	4	3	4
Thalamus and hypothalamus						
Reticular thalamic nucleus	4	4	4	4	4	4
Ventrolateral thalamic nucleus	4	4	3	4	4	4
Ventral anterior thalamic nucleus	4	4	1	4	4	4
Ventral posteromedial/posterolateral thalamic nucleus	4	4	2	4	1	3
Lateral hypothalamic area	4	4	3	4	3	3
Mesencephalic basal ganglia						
Substantia nigra pars compacta	4	4	2	4	1	4
Substantia nigra pars reticulata	4	4	1	4	2	4
White matter tracts						
Olfactory bulb anterior commissure	1	1	1	1	1	1
Ipsilateral forceps minor corporis callosi	4	4	4	4	4	4
Ipsilateral corpus callosum	4	4	4	4	4	4
Contralateral corpus callosum	4	4	4	4	4	4
Anterior commissure	1	4	2	4	1	1
External capsule	4	4	4	4	4	4
Internal capsule	4	4	4	4	4	4
Cerebral peduncle	4	4	1	4	4	4

The axonal outgrowth pattern was analyzed 4 wk after transplantation of differentiated H9 hES cells, A6 non-PDiPS cells and the PDiPS cell lines K1, S1, FF 17–5, and FF 21–26 into the dorsolateral striatum. The code is as follows: 1: 1–5 $hNCAM^+$ fibers per area in 40-μm sections; 2: 6–10 fibers per area in 40-μm sections; 3: 11–20 fibers per area in 40-μm sections; 4: >20 fibers per area in 40-μm sections.

Table S2. Antibodies used for immunostaining procedures

Antibody	Species	Company	Dilution	Comments
hNCAM	Mouse	Santa Cruz Biotechnology	1:100	Human-specific
hL1	Mouse	Neomarkers	1:100	Human-specific
βIII-tubulin	Mouse/rabbit/chicken	Covance	1:1,000	—
TH	Rabbit/sheep	Pel-Freez	1:1,000	—
GFAP	Rabbit	Dako	1:1,000	—
Iba-1	Rabbit	Wako	1:100	—
Calbindin	Mouse	Swant	1:2,000	—
Girk-2	Rabbit	Alamone	1:80	—
Foxa2	Goat	Santa Cruz Biotechnology	1:100	—
GABA	Rabbit	Sigma	1:5,000	—
Nkx2.1	Rabbit	Santa Cruz Biotechnology	1:100	—
DBH	Rabbit	Pel-Freez	1:250	—
Ki-67	Rabbit	Vector	1:1,000	—
α-Synuclein	Mouse	Invitrogen	1:500	LB509 antibody; human-specific
Ubiquitin	Rabbit	Dako	1:500	—
Bhlhb5	Goat	Santa Cruz Biotechnology	1:500	—
Oct4	Mouse	Santa Cruz Biotechnology	1:50	—
SSEA-4	Mouse	DSHB Iowa	3 μg/mL	Clone MC-813